

## 9.3 $\mu\text{m}$ 脉冲 $\text{CO}_2$ 激光辐照牙硬组织的消融特性研究

薛建伟<sup>1</sup>, 吴灵锦<sup>1</sup>, 石晓卫<sup>1</sup>, 黄靖<sup>2</sup>, 梁航<sup>1</sup>, 张先增<sup>1\*</sup>

<sup>1</sup> 福建师范大学光电与信息工程学院, 医学光电科学与技术教育部重点实验室, 福建省光子技术重点实验室, 福建 福州 350007;

<sup>2</sup> 福建医科大学口腔医学院, 福建医科大学附属口腔医院, 福建 福州 350007

**摘要** 波长是生物组织激光消融必须考虑的首要因素。本文以 9.3  $\mu\text{m}$   $\text{CO}_2$  激光为实验光源, 以离体黄种人牙硬组织作为实验样品, 开展了激光消融特性和光剂量学实验研究, 获得了该波长激光辐照牙釉质与牙本质的消融阈值, 评估了消融弹坑的表面形貌、几何尺寸、消融率、消融效率等消融特性与能量密度的相关性。实验结果表明: 9.3  $\mu\text{m}$   $\text{CO}_2$  激光辐照牙釉质的消融阈值大于其辐照牙本质的消融阈值; 牙本质与牙釉质的消融深度、消融直径、消融率均随能量密度增大呈递增变化; 当激光频率为 500 Hz、能量密度为 106.10  $\text{J}/\text{cm}^2$  时, 消融率达到最高, 且牙本质与牙釉质无明显的碳化迹象。本研究结果对该波长激光的临床应用具有一定的参考价值。

**关键词** 激光技术;  $\text{CO}_2$  激光; 激光消融效应; 消融特性; 牙科激光; 能量密度

中图分类号 R318.51

文献标志码 A

DOI: 10.3788/CJL202249.1507105

### 1 引言

利用激光的消融效应可以实现牙硬组织的切割与磨削, 而且切割和磨削的效果可与牙科高速手机等传统切割工具相媲美。生物组织激光消融具有诸多优势: 1) 高能量激光束具有高温杀菌作用, 与组织作用后产生热凝固, 能有效减少出血, 降低术后并发症的可能性; 2) 激光非接触手术方式可以实现任意复杂形状的精确切割, 还可以避免传统切割工具产生的机械损伤, 减轻患者痛苦<sup>[1-4]</sup>。激光消融技术在牙齿备洞、龋齿去除等<sup>[5-6]</sup> 牙科手术中具有广阔的应用前景。

研究表明: 影响生物组织激光消融效应的因素很多, 其中波长是最重要的因素之一。生物硬组织在 9~11  $\mu\text{m}$ 、6~7  $\mu\text{m}$  和 3  $\mu\text{m}$  波长处具有极高的吸收峰。光在上述波段具有以下特点: 1) 光的吸收系数高, 组织表面的光散射和折射引起的能量损耗微不足道; 2) 光的穿透深度小, 组织吸收的光能量可集中分布在组织表面很浅的一层, 消融精确度高, 热损伤小。国内外研究人员已针对不同波长的激光展开研究<sup>[7-13]</sup>, 评估了其对于牙硬组织的消融特性, 如: Apel 等<sup>[8]</sup> 探究了 Er:YAG (2.94  $\mu\text{m}$ )、Er,Cr:YSGG (2.78  $\mu\text{m}$ ) 激光对离体人牙釉质与牙本质的消融特性, 并得到了这两种激光对牙硬组织的消融阈值; 林琪等<sup>[11]</sup> 研究了 Er,Cr:YSGG 激光照射人牙本质的表层晶体结构, 结果发现, 激光消融人牙本质后, 无机物相没有改变, 羟基磷灰石 (HA) 晶粒没有发生重结晶; 江健涛等<sup>[12]</sup> 进行

了子脉冲序列模式 Er:YAG 激光消融牙本质的实验, 结果发现, 在相同的激光脉冲能量下, 较窄的子脉冲宽度可以增加消融量, 降低牙髓腔的温升, 并获得更好的消融坑洞形貌; Almekhdi 等<sup>[13]</sup> 对比了牙骨质经 Er:YAG 激光和  $\text{CO}_2$  激光 (10.6  $\mu\text{m}$ ) 辐照后的表面形貌与微结构, 结果发现, Er:YAG 激光辐照的牙骨质表面出现了轻微烧蚀, 且热损伤较小, 而  $\text{CO}_2$  激光辐照的牙骨质表面出现了明显的碳化, 且热损伤较严重。相关研究发现, 9.3  $\mu\text{m}$   $\text{CO}_2$  激光会被牙组织内的磷灰石剧烈吸收 (吸收系数比其对 Er:YAG 等激光的吸收系数大一个数量级), 吸收的能量通过热传导的方式传递给周围的组织、体液 (主要是水和胶原), 使其汽化, 继而发生“微爆”现象, 最终导致消融的发生。文献<sup>[14-20]</sup> 的研究表明, 采用 9.3  $\mu\text{m}$   $\text{CO}_2$  激光照射牙齿, 不仅可以提高牙齿的耐酸性, 增强氟化物对牙齿的防龋效果, 还可以增强复合树脂材料与牙齿的结合强度。目前, 该波长激光在生物硬组织消融方面表现出了许多独特的优点, 但有关生物硬组织激光消融特性和光剂量学方面的研究还未见系统的评估报道, 而且人牙组织激光消融的相关数据还相对匮乏。鉴于此, 本文以离体黄种人牙硬组织 (牙釉质与牙本质) 为实验对象, 以 9.3  $\mu\text{m}$   $\text{CO}_2$  激光为实验光源, 开展激光消融特性和光剂量学实验研究, 获得该波长激光辐照牙釉质与牙本质的消融阈值, 评估能量密度对消融弹坑表面形貌、几何尺寸、消融率、消融效率的影响。本文的研究成果

收稿日期: 2021-11-02; 修回日期: 2021-12-13; 录用日期: 2022-01-17

基金项目: 国家自然科学基金 (61575042)、福建省自然科学基金 (2019J012850, 2020J01156)

通信作者: \*xzhang@fjnu.edu.cn

可为该激光器的临床应用提供基础数据和参考依据。

## 2 材料与方法

实验样品来自福建医科大学附属口腔医院提供的因医学原因拔除的牙根发育完全的黄种人恒磨牙,样品无龋坏、根裂等缺陷,无填充体,未做过牙髓治疗。获得样品后,首先清除附着的牙结石、牙菌斑等异物;然后用慢速金刚锯在喷水冷却下沿牙体长轴方向将样品切成 4 部分,共获得 40 个包含完整牙釉质和牙本质的纵切面样品 ( $n = 40$ ),每个样品至少包含  $5 \text{ mm} \times 5 \text{ mm}$  的完整牙本质部分与  $3 \text{ mm} \times 3 \text{ mm}$  的完整牙釉质部分;随后将切面用 180 目石英砂纸打磨,保证样品表面的平滑度;用清水清洗样品,然后将其保存于生理盐水中,并在 1 个月内用于实验。

实验光源为深圳大通激光有限公司生产的脉冲  $\text{CO}_2$  激光器,型号为 DL-500,其输出激光的波长为  $9.3 \mu\text{m}$ ,脉宽在  $5 \sim 25 \mu\text{s}$  之间,峰值功率在  $228 \sim 648 \text{ W}$  之间,激光束聚焦于组织样品上的光斑直径约为  $120 \mu\text{m}$ ,输出能量在  $1.1 \sim 16.2 \text{ mJ/pulse}$  内可调。激光消融实验装置如图 1 所示,将制备好的牙齿切面固定于升降平台上, $\text{CO}_2$  激光束经振镜装置聚焦于组织样品表面,激光能量通过能量计(表头型号:NOVA II;探头型号:PE5O-BB-SH-V2)进行实时监测。辐照时,外置水喷雾系统开启,均匀喷射于激光聚焦点处。

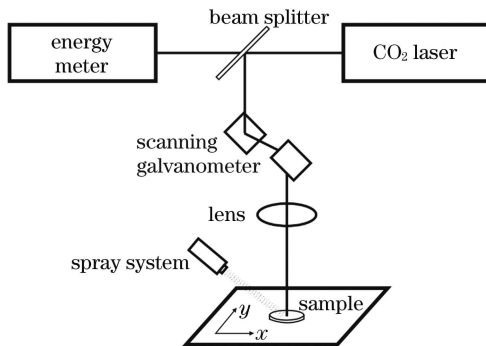


图 1 牙硬组织激光消融实验装置图

Fig. 1 Experimental setup of tooth hard tissue laser ablation

根据辐照条件,将实验样本随机分为 A、B 两组。A 组 ( $n = 20$ ):在不喷水的条件下,单个激光脉冲分别以  $4.23, 4.61, 5.05, 5.56, 5.84, 6.14, 6.83, 7.69 \text{ J/cm}^2$  的能量密度依次辐照每个样本上的牙本质与牙釉质,探究激光对牙本质与牙釉质的消融阈值;B 组 ( $n = 20$ ):分别以  $9.73, 37.14, 65.43, 88.42, 106.10 \text{ J/cm}^2$  的能量密度,在无喷水与水喷雾(水流速为  $0.25 \text{ mL/s}$ )环境下,对牙本质与牙釉质进行单脉冲辐照,探究不同激光能量密度对牙本质与牙釉质的消融特性。激光辐照结束后,采用数码显微镜(型号:VHX-970F)观察并拍摄样本图像,图像经处理后可用于表面形貌分析。将样品表面出现弹坑或组织去除的现象视为消融发生,并用软件测量消融弹坑的直径、深度和体积。这里定义消融概率为  $80\%$  对应的能量密度为消融阈值,单位能量激光下的消融深度为消融效率,单位时间内的消融体积为消融率。由于单个脉冲的时间测量误差较大,故本文采用线扫描(线长为  $0.9 \text{ mm}$ ,扫描速度为  $60 \text{ mm}^2/\text{s}$ ,频率为  $500 \text{ Hz}$ )下的消融体积与所用时间之比表示消融率。

## 3 结果与讨论

### 3.1 消融阈值

消融阈值指消融概率为  $80\%$  对应的能量密度。在实验用激光器提供的参数范围内,牙组织表面均可产生明显的消融现象。故,选取峰值功率为  $228 \text{ W}$ 、脉宽为  $5 \mu\text{s}$ (能量密度为  $9.73 \text{ J/cm}^2$ ) 的激光参数,通过调节光斑尺寸获得 8 组能量密度值 ( $4.23, 4.61, 5.05, 5.56, 5.84, 6.14, 6.83, 7.69 \text{ J/cm}^2$ ),探究  $9.3 \mu\text{m}$   $\text{CO}_2$  激光对牙硬组织的消融阈值。

图 2 所示为  $\text{CO}_2$  激光以较低能量密度辐照牙硬组织产生的消融弹坑的三维合成图。图中的不同颜色代表不同深度,颜色-深度对应关系在每个图的左侧标注出,这种关系在每个图中不尽相同。如图 2(a)、(e) 所示,当激光能量密度为  $5.05 \text{ J/cm}^2$  时,牙本质与牙釉质表面仅有轻微的消融痕迹产生,且消融效果较弱

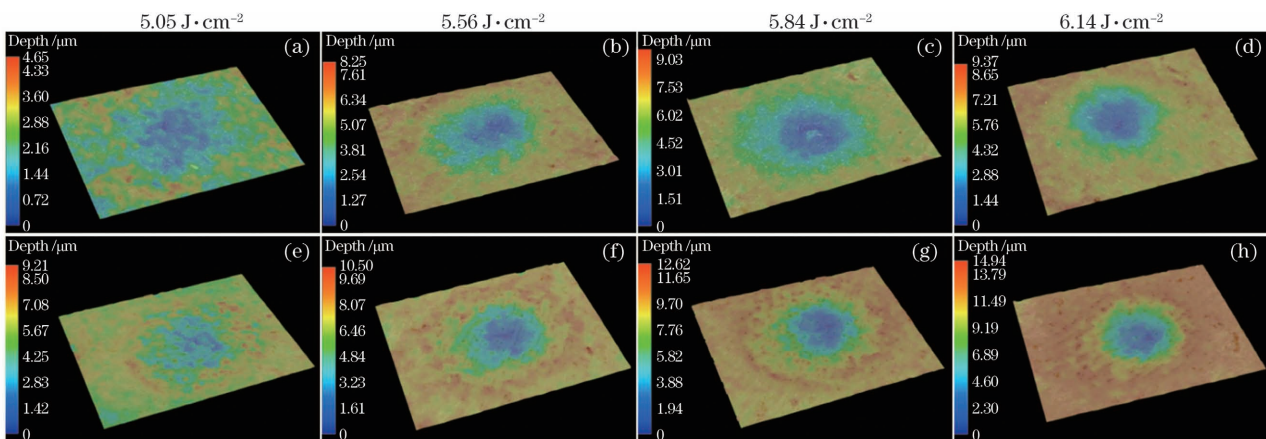


图 2 激光辐照牙硬组织消融弹坑的三维合成图。(a)~(d)牙釉质消融弹坑;(e)~(h)牙本质消融弹坑

Fig. 2 Three-dimensional composite images of ablation craters in hard tooth tissues irradiated by laser. (a)~(d) Ablation crater in enamel; (e)~(h) ablation crater in dentin



(深度小于  $5\ \mu\text{m}$ ),未能成功消融。此时,20 个样本中只有 1 处牙釉质(5%)和 2 处牙本质(10%)判定为成功消融,消融概率低于 80%。随着能量密度增加,牙釉质与牙本质的消融深度有了一定增加,如图 2(d)、(h)所示,当能量密度为  $6.14\ \text{J}/\text{cm}^2$  时,牙釉质与牙本质表面出现了显著的消融痕迹,20 个样本中有 18 处牙釉质(90%)和 19 处牙本质(95%)判定为成功消融,消融概率超过 80%。综上, $9.3\ \mu\text{m}\ \text{CO}_2$  激光对牙釉质与牙本质的消融阈值在  $5.05\sim 6.14\ \text{J}/\text{cm}^2$  之间。

将上述实验结果使用统计软件(SPSS 24.0)的

概率功能进行回归分析,获得如图 3 所示的消融发生概率统计图。由图 3 可知, $9.3\ \mu\text{m}\ \text{CO}_2$  激光对牙釉质的消融阈值为  $6.07\ \text{J}/\text{cm}^2$ ,对牙本质的消融阈值为  $5.76\ \text{J}/\text{cm}^2$ 。激光辐照牙釉质的消融阈值略大于其辐照牙本质的消融阈值,这是因为牙釉质富含矿物质(占比 95%),矿物质由熔点较高的羟基磷灰石组成,不易去除,故而消融阈值相对较高;而牙本质的矿物质含量相对较低(占比 70%),且结构稀疏多孔、富含牙本质小管,因此牙本质更容易被去除,消融阈值相对较低。

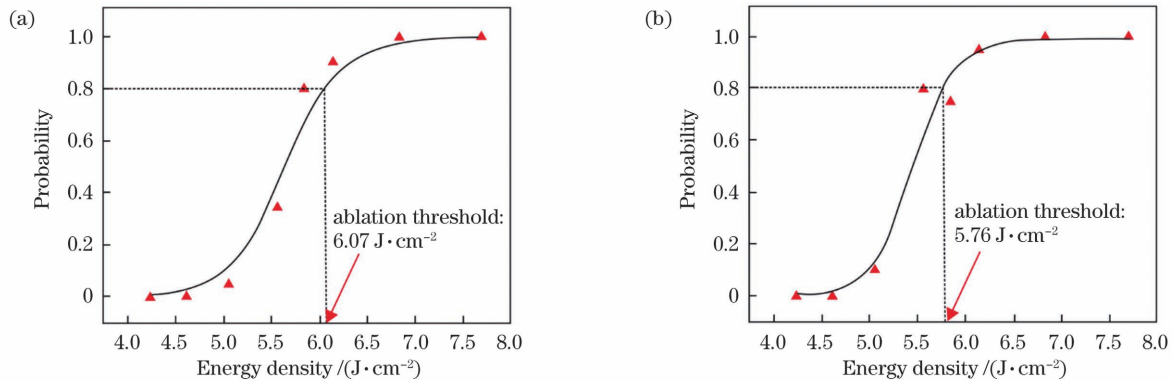


图 3  $9.3\ \mu\text{m}\ \text{CO}_2$  激光辐照牙硬组织消融发生概率统计图。(a)牙釉质;(b)牙本质

Fig. 3 Statistical charts of occurrence probability of ablation of hard tooth tissues irradiated by  $\text{CO}_2$  laser with  $9.3\ \mu\text{m}$  wavelength. (a) Enamel; (b) dentin

### 3.2 弹坑表面形貌分析

激光以  $106.10\ \text{J}/\text{cm}^2$  的能量密度辐照牙硬组织产生的消融弹坑的俯视图、三维合成图、截面图如图 4 所示。由图 4 可见:消融凹陷呈倒圆锥状,其截面近似于抛物线;从俯视图来看,弹坑呈近圆形,圆形弹坑与周围组织的边界清晰。本实验采用的  $9.3\ \mu\text{m}$  激光束能量在焦平面上呈高斯分布,即中心能量最高,四周能量递减,中间区域能量密度超过阈值发生消融,周围则

没有消融,因此弹坑呈近圆形。激光消融牙本质产生了规则平整的光滑侧面,弹坑内牙本质小管清晰可见,而牙釉质的消融弹坑呈鳞片状。牙釉质和牙本质的消融弹坑内均未发生碳化现象且无碎屑存在。这是因为本实验采用的激光脉宽( $5\sim 25\ \mu\text{s}$ )小于牙硬组织的热弛豫时间,满足热局限条件,热能基本局限在辐射范围内,因而单个激光脉冲即使以高能量密度辐照牙硬组织,其表面依旧不会出现碳化现象。

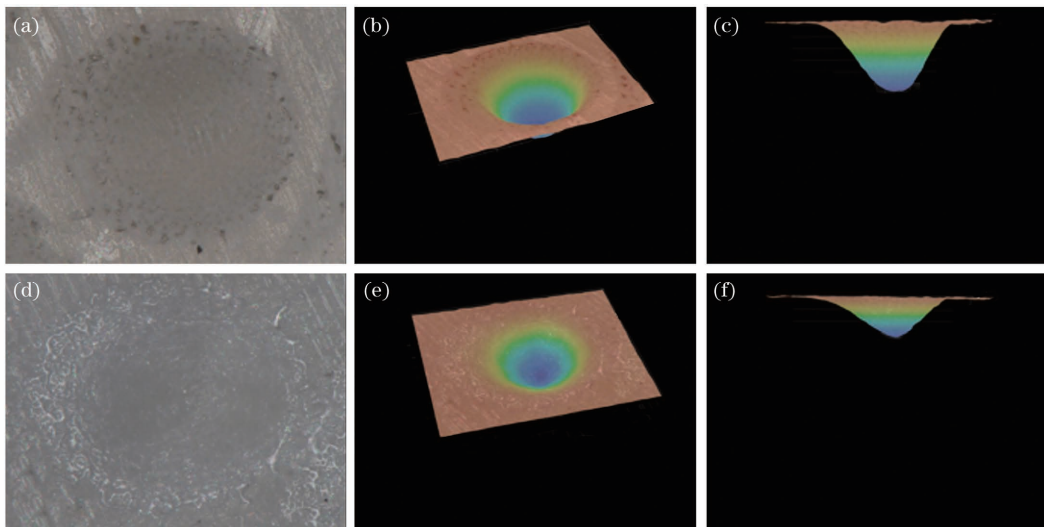


图 4 激光以  $106.10\ \text{J}/\text{cm}^2$  的能量密度辐照牙硬组织产生的消融弹坑的俯视图、三维合成图及截面图。(a)~(c)牙本质;(d)~(f)牙釉质

Fig. 4 Top views, three-dimensional composite images, and cross-sectional views of hard tooth tissues ablation craters irradiated by laser with energy density of  $106.10\ \text{J}/\text{cm}^2$ . (a)~(c) Dentin; (d)~(f) enamel

### 3.3 弹坑几何尺寸

图 5 所示为激光辐照牙硬组织产生的消融弹坑深度、直径随能量密度的变化。由图 5 可知,牙本质与牙釉质表面的弹坑深度与直径均随能量密度增大呈递增趋势,激光能量密度对消融弹坑几何尺寸具有显著影

响。在相同的能量密度下,激光对牙本质的消融深度显然大于对牙釉质的消融深度,且随着能量密度增大,牙本质与牙釉质消融深度的差距增大。虽然本实验中的光斑直径仅为  $120\ \mu\text{m}$ ,但各能量密度下的弹坑直径均大于光斑直径。

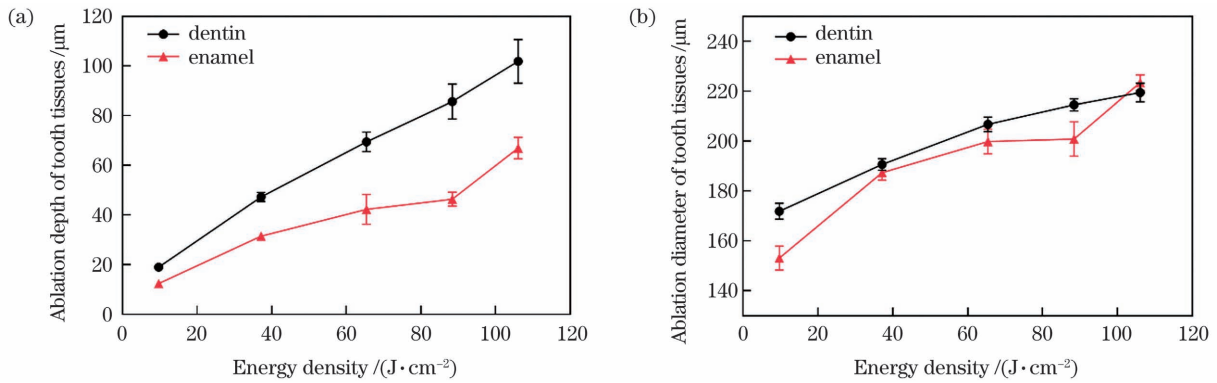


图 5 激光辐照牙硬组织产生的消融弹坑的几何尺寸随能量密度的变化。(a)消融深度随能量密度的变化;(b)消融直径随能量密度的变化

Fig. 5 Variation of geometric size of ablation craters produced by laser irradiating hard tooth tissues with energy density.

(a) Variation of ablation depth with energy density; (b) variation of ablation diameter with energy density

### 3.4 消融效率与消融率

消融效率与消融率是表征激光消融特性的两个重要参量。图 6 为激光辐照牙硬组织的消融效率随能量密度的变化。在无喷水环境下,  $9.3\ \mu\text{m}\ \text{CO}_2$  激光对牙釉质的消融效率(均值)随着能量密度增大呈先递减后递增的趋势,对牙本质的消融效率(均值)随着能量密度增大呈递减的趋势。这可能与  $9.3\ \mu\text{m}$  激光的消融机制有关,即:牙硬组织内的羟基磷灰石吸收激光能量后,将能量传递给水,引起内建压力增大,产生“微爆”效应,导致组织去除(硬组织的“双组分”消融机制)。牙釉质消融效率在  $88.42\ \text{J}/\text{cm}^2$  的能量密度下出现了拐点,这可

能与牙釉质内大量的羟基磷灰石含量有关,本课题组后续将对其原因展开进一步实验探究。此次实验还发现,能量密度高于  $106.10\ \text{J}/\text{cm}^2$  后,牙本质与牙釉质的消融效率继续呈递减趋势。另外,相关研究表明,激光结合水喷雾可以有效降低牙组织温升,避免碳化现象出现,但从图 6 所示的喷水实验结果来看,在低能量密度下,单个激光脉冲对牙釉质与牙本质的消融效率与无喷水环境下的相比反而降低。这可能是因为消融弹坑中大部分能量被水雾吸收,使得此时的消融效率降低。随着能量密度增大,水雾对消融效率的影响逐渐减小,有无喷水环境下消融效率的差值逐渐缩小。

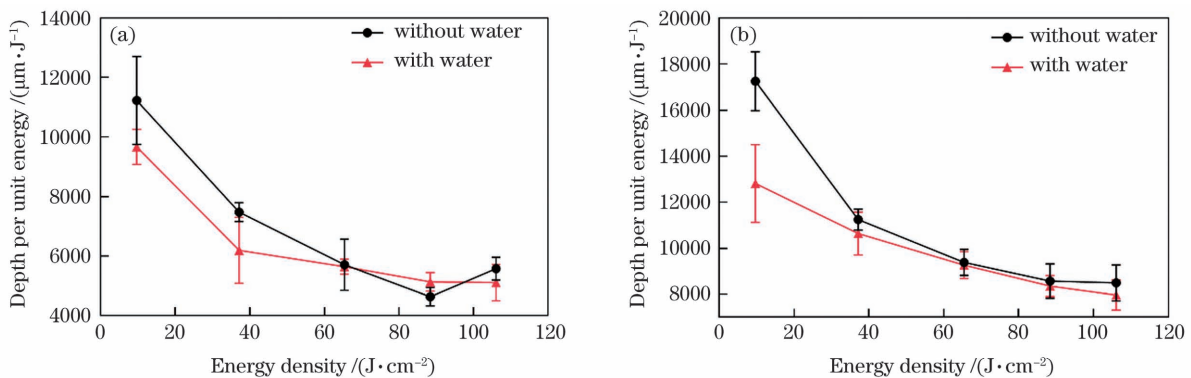


图 6 激光辐照牙硬组织的消融效率随脉冲能量密度的变化关系。(a)牙釉质;(b)牙本质

Fig. 6 Variation of ablation efficiency of laser-irradiated tooth hard tissues with pulse energy density. (a) Enamel; (b) dentin

图 7 为激光辐照牙硬组织的消融率随能量密度的变化。由图 7 可知,  $9.3\ \mu\text{m}\ \text{CO}_2$  激光对牙釉质与牙本质的消融率均随能量密度增大呈递增趋势,并且在能量密度为  $106.10\ \text{J}/\text{cm}^2$  (激光频率为  $500\ \text{Hz}$ ) 时达到最高,分别为  $(0.308 \pm 0.026)\ \text{mm}^3/\text{s}$  和  $(0.510 \pm 0.032)\ \text{mm}^3/\text{s}$ 。当激光频率为  $50\ \text{Hz}$  时,激光器的能

量密度最大 ( $143.24\ \text{J}/\text{cm}^2$ ),但此时的消融时间延长,消融率反而降低了。因此,激光器以  $500\ \text{Hz}$  频率、 $106.10\ \text{J}/\text{cm}^2$  的能量密度消融牙硬组织可得到最大的消融率。虽然这与牙科手机等传统器械的消融率(最低  $1\ \text{mm}^3/\text{s}$ )相比还有一定差距,但相比其他常用牙硬组织消融激光快了许多。由于牙釉质与牙本质的

结构差异,在相同的能量密度下,激光对牙本质的消融体积始终高于对牙釉质的消融体积,故激光对牙本质的消融率高于对牙釉质的消融率。

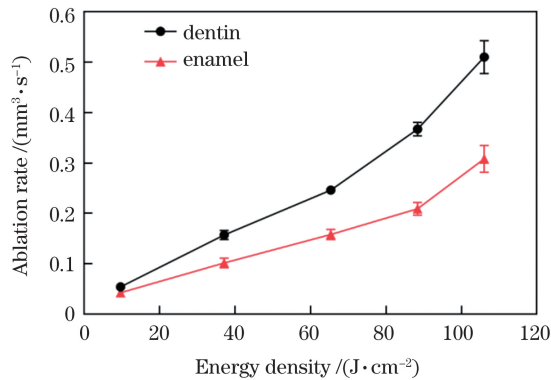


图 7 激光辐照牙硬组织的消融率随能量密度的变化

Fig. 7 Variation of ablation rate of laser-irradiated tooth hard tissues with energy density

## 4 结 论

激光在生物硬组织消融领域具有广阔的应用前景,激光的出现革新了传统牙科治疗方式,在牙齿备洞、龋齿去除等硬组织手术中成为一种常规性治疗手段。本文系统评估了  $9.3 \mu\text{m}$   $\text{CO}_2$  激光辐照牙硬组织(牙釉质与牙本质)的消融特性,获得了该波长激光辐照牙釉质与牙本质的消融阈值,比较了消融弹坑的几何尺寸(消融弹坑直径与深度)、消融效率、消融率随能量密度的变化。实验结果表明: $9.3 \mu\text{m}$  激光辐照牙釉质的消融阈值大于其辐照牙本质的消融阈值,牙本质与牙釉质的消融深度、消融直径、消融率均随能量密度增大呈递增变化,当能量密度为  $106.10 \text{ J/cm}^2$ 、激光频率为  $500 \text{ Hz}$  时,消融率达到最大,且无明显的碳化迹象。本研究成果有助于进一步理解生物硬组织的消融机制,获得的消融阈值和光剂量学特性参数有望为该技术的临床应用提供基础数据和参考依据。

## 参 考 文 献

- [1] Blaskovic M, Gabrić D, Coleman N J, et al. Bone healing following different types of osteotomy: scanning electron microscopy (SEM) and three-dimensional SEM analyses [J]. *Microscopy and Microanalysis*, 2016, 22(6): 1170-1178.
- [2] Aleksic V, Aoki A, Iwasaki K, et al. Low-level Er:YAG laser irradiation enhances osteoblast proliferation through activation of MAPK/ERK [J]. *Lasers in Medical Science*, 2010, 25(4): 559-569.
- [3] Sasaki K M, Aoki A, Ichinose S, et al. Ultrastructural analysis of bone tissue irradiated by Er:YAG Laser [J]. *Lasers in Surgery and Medicine*, 2002, 31(5): 322-332.
- [4] Stübinger S, Biermeier K, Bächli B, et al. Comparison of Er:YAG laser, piezoelectric, and drill osteotomy for dental implant site preparation: a biomechanical and histological analysis in sheep [J]. *Lasers in Surgery and Medicine*, 2010, 42(7): 652-661.
- [5] Braun A, Krillke R F, Frentzen M, et al. Heat generation caused by ablation of dental hard tissues with an ultrashort pulse laser (USPL) system [J]. *Lasers in Medical Science*, 2015, 30

- (2): 475-481.
- [6] 丁一, 肖诗梦, 杨恒, 等. Nd:YAG 激光在口腔医学中的应用 [J]. *华西口腔医学杂志*, 2015, 33(5): 445-450.
- [7] Ding Y, Xiao S M, Yang H, et al. Application of Nd:YAG laser in stomatology [J]. *West China Journal of Stomatology*, 2015, 33(5): 445-450.
- [7] 张先增. 脉冲激光诱导生物硬组织消融及其医疗新技术 [D]. 福州: 福建师范大学, 2010: 23.
- [8] Zhang X Z. Hard biotissue ablation with pulse lasers and its novel medical technology [D]. Fuzhou: Fujian Normal University, 2010: 23.
- [8] Apel C, Meister J, Ioana R S, et al. The ablation threshold of Er:YAG and Er:YSGG laser radiation in dental enamel [J]. *Lasers in Medical Science*, 2002, 17(4): 246-252.
- [9] Hibst R, Keller U. Experimental studies of the application of the Er:YAG laser on dental hard substances: I. Measurement of the ablation rate [J]. *Lasers in Surgery and Medicine*, 1989, 9(4): 338-344.
- [10] Belikov A V, Erofeev A V, Shumilin V V, et al. Comparative study of the  $3 \mu\text{m}$  laser action on different hard tooth tissue samples using free running pulsed Er-doped YAG, YSGG, YAP and YLF lasers [J]. *Proceedings of SPIE*, 1993, 2080: 60-67.
- [11] 林琪, 林昱, 谢云德, 等. 基于 X 射线衍射的激光消融改变人牙本质表层晶体结构的研究 [J]. *激光与光电子学进展*, 2020, 57(23): 231701.
- [12] Lin Q, Lin Y, Xie Y D, et al. Study on crystal structure change of laser-ablated human dentin surface based on X-ray diffraction [J]. *Laser & Optoelectronics Progress*, 2020, 57(23): 231701.
- [12] 江健涛, 魏蒙恩, 熊正东, 等. 子脉冲序列模式 Er:YAG 激光消融牙本质的实验观察 [J]. *中国激光*, 2021, 48(1): 0107001.
- [13] Jiang J T, Wei M E, Xiong Z D, et al. Observation of dentin ablation using an Er:YAG laser in a sub-pulse sequence mode [J]. *Chinese Journal of Lasers*, 2021, 48(1): 0107001.
- [14] Almhedi A, Aoki A, Ichinose S, et al. Histological and SEM analysis of root cementum following irradiation with Er:YAG and  $\text{CO}_2$  lasers [J]. *Lasers in Medical Science*, 2013, 28(1): 203-213.
- [15] Fried D, Zuerlein M J, Le C Q, et al. Thermal and chemical modification of dentin by 9-11-microm  $\text{CO}_2$  laser pulses of 5-100-micros duration [J]. *Lasers in Surgery and Medicine*, 2002, 31(4): 275-282.
- [16] Takahashi K, Kimura Y, Matsumoto K. Morphological and atomic analytical changes after  $\text{CO}_2$  laser irradiation emitted at  $9.3 \mu\text{m}$  on human dental hard tissues [J]. *Journal of Clinical Laser Medicine & Surgery*, 1998, 16(3): 167-173.
- [17] Badreddine A H, Couitt S, Donovan J, et al. Demineralization inhibition by high-speed scanning of  $9.3 \mu\text{m}$   $\text{CO}_2$  single laser pulses over enamel [J]. *Lasers in Surgery and Medicine*, 2021, 53(5): 703-712.
- [18] Lee R, Chan K H, Jew J, et al. Synergistic effect of fluoride and laser irradiation for the inhibition of the demineralization of dental enamel [J]. *Proceedings of SPIE*, 2017, 10044: 100440L.
- [19] Hsu D J, Darling C L, Lachica M M, et al. Nondestructive assessment of the inhibition of enamel demineralization by  $\text{CO}_2$  laser treatment using polarization sensitive optical coherence tomography [J]. *Journal of Biomedical Optics*, 2008, 13(5): 054027.
- [20] Rechmann P, Sherathiya K, Kinsel R, et al. Influence of irradiation by a novel  $\text{CO}_2$   $9.3\text{-}\mu\text{m}$  short-pulsed laser on sealant bond strength [J]. *Lasers in Medical Science*, 2017, 32(3): 609-620.
- [21] Rechmann P, Bartolome N, Kinsel R, et al. Bond strength of etch-and-rinse and self-etch adhesive systems to enamel and dentin irradiated with a novel  $\text{CO}_2$   $9.3 \mu\text{m}$  short-pulsed laser for dental restorative procedures [J]. *Lasers in Medical Science*, 2017, 32(9): 1981-1993.



# Ablation Characteristics of Hard Tooth Tissues Irradiated by 9.3 $\mu\text{m}$ CO<sub>2</sub> Laser

Xue Jianwei<sup>1</sup>, Wu Lingjin<sup>1</sup>, Shi Xiaowei<sup>1</sup>, Huang Jing<sup>2</sup>, Liang Hang<sup>1</sup>, Zhang Xianzeng<sup>1\*</sup>

<sup>1</sup> College of Photonic and Electronic Engineering, Fujian Normal University, Key Laboratory of Opto-Electronic Science and Technology for Medicine of Ministry of Education, Fujian Provincial Key Laboratory of Photonics Technology, Fuzhou 350007, Fujian, China;

<sup>2</sup> School and Hospital of Stomatology, Fujian Medical University, Fuzhou 350007, Fujian, China

## Abstract

**Objective** Laser ablation effect can be used to cut and grind the hard tooth tissues, thereby offering several advantages over traditional instruments. As a result, laser ablation technology is applicable to various dental procedures. The ablation effect of lasers on hard biological tissues is highly dependent on wavelength. As is well known, the erbium-doped yttrium aluminum garnet (Er:YAG) laser is the most frequently used dental laser because its wavelength is close to the strong absorption peaks of water and hydroxyapatite. However, this wavelength laser has a low ablation rate and must be used in conjunction with water spray. According to previous research, the 9.3  $\mu\text{m}$  CO<sub>2</sub> laser has a higher absorption coefficient for apatite than the Er:YAG laser and offers a number of unique advantages when it comes to biological hard tissue ablation. For example, irradiating teeth with a CO<sub>2</sub> laser at a wavelength of 9.3  $\mu\text{m}$  can improve their acid resistance, increase the anticaries effect of fluoride on teeth, and strengthen the bond between composite resin materials and teeth. However, there is currently no systematic evaluation report on the ablation characteristics of this wavelength laser on biological hard tissues, and data on the ablation of human dental tissue is also sparse.

**Methods** Experimental samples were randomly assigned to the A and B groups. In group A (the quantity of samples  $n = 20$ ), without spraying water, a single laser pulse irradiated the dentin and enamel on each sample with energy densities of 4.23, 4.61, 5.05, 5.56, 5.84, 6.14, 6.83, and 7.69 J/cm<sup>2</sup> to determine the dentin and enamel laser ablation thresholds. In group B ( $n = 20$ ), to investigate the ablation characteristics of various energy densities, a single laser pulse irradiated the dentin and enamel with energy densities of 9.73, 37.14, 65.43, 88.42, and 106.10 J/cm<sup>2</sup> under water spray (water flow rate of 0.25 mL/s) and non-water spray conditions. Following laser irradiation, the experimental samples were observed and photographed using a digital microscope. We defined the ablation threshold as the energy density that corresponds to 80% of the ablation probability, the ablation efficiency as the depth of ablation per unit of energy, and the ablation rate as the volume of ablation per unit time. Due to the relatively large time measurement error associated with a single pulse, the ablation rate in this study was expressed as the ratio of the measured volume to the elapsed time represented by the line scan (line length is 0.9 mm, scan speed is 60 mm<sup>2</sup>/s, and frequency is 500 Hz).

**Results and Discussions** Due to the composition and structure of dentin and enamel, the ablation threshold of the 9.3  $\mu\text{m}$  CO<sub>2</sub> laser is greater for enamel (6.07 J/cm<sup>2</sup>) than that of dentin (5.76 J/cm<sup>2</sup>) (Fig. 3). Additionally, we discovered that the energy density of the pulse has a significant effect on the ablation characteristics of hard tooth tissues. On the one hand, as energy density increases, both the geometric size of the ablation crater and the rate of ablation increase (Fig. 5, Fig. 7). Moreover, the dentin and enamel laser ablation rates reach their maximum values when the energy density reaches 106.10 J/cm<sup>2</sup> and the frequency is 500 Hz, and the maximum values are  $(0.308 \pm 0.026)$  mm<sup>3</sup>/s and  $(0.510 \pm 0.032)$  mm<sup>3</sup>/s, respectively. The crater created by the 106.10 J/cm<sup>2</sup> laser energy density is inverted cone-shaped and noncarbonized, but the surface morphologies of dentin and enamel are different (Fig. 4). On the other hand, the mean value of laser ablation efficiency of dentin decreases as the energy density increases, whereas the mean value of laser ablation efficiency of enamel initially decreases and then increases as the energy density increases (Fig. 6).

**Conclusions** To the best of our knowledge, this is the first study to investigate the ablation characteristics of hard tooth tissues (enamel and dentin) using a 9.3  $\mu\text{m}$  CO<sub>2</sub> laser. In this work, we determined the ablation threshold of enamel and dentin exposed to the wavelength of the laser and subsequently investigated the relationship between ablation crater geometry, ablation efficiency, and ablation rate as a function of energy density. The experimental results indicate that the ablation threshold of 9.3  $\mu\text{m}$  wavelength laser-irradiated tooth enamel is greater than the ablation threshold of laser-irradiated dentin. Additionally, the ablation depth, ablation diameter, and ablation rate of irradiated dentin and enamel increase in direct proportion to the energy density. Moreover, when the energy density is 106.10 J/cm<sup>2</sup> and the laser frequency is 500 Hz, the ablation rate reaches its maximum, with no obvious sign of carbonization. The research findings will contribute significantly to a better understanding of the biohard tissue ablation mechanism, and the ablation threshold and photodosimetry characteristic parameters obtained from our study will thereby serve as a foundation for promoting the clinical application of this technology.

**Key words** laser technique; CO<sub>2</sub> laser; laser ablation effect; ablation characteristics; dental laser; energy density